# Mathematica Balkanica

Mathematical Society of South-Eastern Europe
A quarterly published by
the Bulgarian Academy of Sciences – National Committee for Mathematics

---

New Series Vol.11, 1997, Fasc. 1-2

# Orthonormal Systems of Fractal Functions [1]

*Bl. Sendov, P. Marinov*

The notion of a fractal function of one variable is introduced as a function defined, bounded and continuous on the set of all binary irrational points of the unit interval. The fractal dimension of a function is defined through the box dimension of its completed graph as a point set on the plane.

An orthonormal system of fractal functions with given fractal dimension is constructed.

Computer experiments for signal compression through fractal transform coding are presented.

## 1. Introduction

The signals and the images are now very popular objects for approximation to accomplish data compression. These objects are not only with local peculiarities, but are also very "rough" and resemble the fractals. It is natural to use fractal structures for approximation of real world signals and images [1], [2], [3], [4], [9], [16]. The technique in this direction is based now on the so called Iterated Function Systems (IFS) [1], [4], which are collections of contractive transformations in given functional spaces. The fixed points of these IFS are fractal functions with self similarity [14], [11], [15] and given fractal dimension [16], [17], [7], [8]. To implement this method, we have to find a suitable transformation, such that its unique fixed point is an useful approximation to a given function representing the target image. This original idea needs an efficient algorithm for finding these "suitable" transformations.

In this paper we propose a new approach to fractal structures, with given fractal dimension, for the purpose of approximation and hence for signal and real world image compression. For simplicity, we consider one-dimensional case of functions defined on the unit interval.

[1]Supported by Contract I-401/94 with Bulgarian National Research Foundation

The first important feature of our study, differing from the already established theory of fractal approximation and interpolation, is that we do not limit ourselves only with continuous functions. To allow the treatment of discontinuous fractal functions, we consider functions defined, bounded and continuous only on the set $(0;0)$ of all binary irrational points in the unit interval $[0,1]$. To every such function $f$ corresponds a so called *completed graph* $F(f)$ [18], which is the smallest compact and convex, in respect to the $y$-axis, point set on the plane containing the graph of the function $f$. This completed graph is used to define the fractal dimension of a function as the box dimension of its completed graph. For example, the Dirichle function

$$D(x) = \begin{cases} 0 & \text{for } x \text{ rational,} \\ 1 & \text{for } x \text{ irrational,} \end{cases} \quad x \in [0,1],$$

has as its completed graph $F(D) = \{(x,y) : 0 \le x \le 1, \ 0 \le y \le 1\}$ the full square, and hence a box dimension 2. It should be noted that the graph of $D$ has a box dimension 1. This definition of the fractal dimension of a discontinuous function is the most natural from the point of view of the Hausdorff distance [12] between functions [18], [19], [22] and it is equivalent to the dimension defined by A. Deliu and B. Jawerth [6, p. 217] for the graph of a general bounded function.

In fact $O = (0;0)$ is a set, dense in $[0,1]$, which is invariant with respect to the collection $\mathcal{J} = \{w_0, w_1\}$ of similitudes $w_0(x) = x/2$, $w_1(x) = (x+1)/2$, such that $O = w_0(O) \cup w_1(O)$ and $w_0(O) \cap w_1(O) = \emptyset$. This reminds us the *open set condition* [14, p. 735] in a stronger form.

Second step is the design of a method for *fractalizing* a given orthogonal system. This method is based on the Weierstrass' idea of producing a function which is continuous but nowhere differentiable [10]. One example of such a function is

$$W_\alpha(t) = \sum_{i=1}^{\infty} \lambda^i \cos(2^i \pi t), \quad 1/2 \le \lambda < 1.$$

For us it is important that this function has a fractal dimension $1+\alpha$ [16], where $\alpha = 1 + \log_2 \lambda$. Our method produces the famous Weierstrass function in the first step if we start to fractalize the orthogonal system $g_n^*(t) = \cos(2^n \pi t)$; $n = 1, 2, 3, \ldots$ . This approach for producing fractal functions is used in [21], [13], [5].

The structure of the paper is as follows.

In section 2 we introduce the notion of a *fractal function* as a function defined on $(0;0)$ - the set of the irrational points in the unit interval. The role of continuity in this setting is played by the Hausdorff continuity [18], [19] and the

classical modulus of continuity $\omega$ has to be replaced by the Hausdorff modulus of continuity $\tau$.

We define the fractal dimension of a bounded function as the dimension of its completed graph [18], [19] and introduce the Hausdorff distances in the space of fractal functions.

An orthonormal base of Haar type, called *Extended Haar system* is introduced in section 3, which is useful for producing orthogonal systems of fractal functions with given fractal dimension.

The section 4 contains the method of fractalization of an arbitrary orthonormal system.

In section 5 the Extended Haar system is fractalized and the connection with the IFS is discussed. The theory of the IFS [1], [2], [3], [4], [9], in the one dimensional case, is based on the contractive mappings of the form

$$w : \begin{pmatrix} x \\ y \end{pmatrix} \to \begin{pmatrix} a & 0 \\ c & s \end{pmatrix} \begin{pmatrix} x \\ y \end{pmatrix} + \begin{pmatrix} d \\ e \end{pmatrix},$$

where $a$ is the contractive factor for the argument, $s$ is the contractive factor for the values of the function and $c$ serves to guarantee the continuity. In our study we consider contractive mappings with $c = 0$, as we do not need continuity.

In section 6 we present some examples of using the fractal transform coding for compression of the graphs of smooth functions and some "rough" functions taken from real images. The quality of the recovery is measured by the $L_1$, $L_2$ norms and integral Hausdorff distance.

In this paper we consider only the one-dimensional case. The same technique works easily also in the multi-dimensional case and shall be presented in another paper with applications in image compression.

## 2. Basic definitions

Every number $x \in (0,1)$ may be represented in the binary form

$$x = a_1(x)2^{-1} + a_2(x)2^{-2} + a_3(x)2^{-3} + \dots , \tag{2.1}$$

where $a_n(x)$ is 0 or 1. The number $x$ is binary irrational, if $a_n(x) = 0$ for infinitely many indices $n$ and $a_n(x) = 1$ for infinitely many indices $n$.

Let $(k;p)$, where $k, p$ are non negative integers and $p < 2^k$, be the set of all binary irrational numbers from the interval $(p2^{-k}, (p+1)2^{-k})$. The set $(k;p)$ is called a *binary interval* of rank $k$. The binary interval $(0;0) \subset [0,1]$ is of rank 0.

The functions $a_n(x)$ from (2.1) are uniquely defined in $(0;0)$.

**Definition 2.1.** We call the function $f$ a *fractal function*, if it is defined, bounded and continuous on the unit binary interval $(0;0)$.

The set of all fractal functions is denoted by $\mathcal{F}_{(0;0)} = \mathcal{F}$.

Every fractal function $f$ from $\mathcal{F}$ is Lebesgue integrable in the interval $[0,1]$ as $f$ is not defined only in the set with measure zero in this interval.

In the functional space $\mathcal{F}$ we shall use the uniform norm

$$\|f\| = \sup\{|f(x)| : x \in (0;0)\},$$

and the integral norms $L_1$ and $L_2$:

$$\|f\|_1 = \int_0^1 |f(x)|\,dx, \quad \|f\|_2 = \left(\int_0^1 f^2(x)\,dx\right)^{\frac{1}{2}}.$$

If $f \in \mathcal{F}$, then for every $x \in [0,1]$ there exist the limits

$$\lim_{h\to 0} \inf f(x+h) = \underline{f}(x) \quad \text{and} \quad \lim_{h\to 0} \sup f(x+h) = \overline{f}(x); \quad x+h \in (0;0).$$

**Definition 2.2.** The *completed graph* $F(f)$ [18] of the function $f$ is the smallest compact and convex, towards the $y$-axis, point set on the plane containing the graph of the function $f$.

The *Hausdorff distance* between two functions $f, g \in \mathcal{F}$ is defined as the Hausdorff distance between their completed graphs as point sets on the plane. For a particular definition of this distance we need to choose a distance between two points in the plane. For our purpose, a convenient distance on the plane is the box distance

$$\rho_p(A(x_1,y_1),\ B(x_2,y_2)) = \max\{|x_1-x_2|,\ p|y_1-y_2|\}, \quad p>0.$$

For simplicity, we shall use $\rho_1 = \rho$.

**Definition 2.3.** The Hausdorff distance between two functions $f, g \in \mathcal{F}$ is the number

$$r(f,g) = \max\left\{\sup_{A\in F(f)} \inf_{B\in F(g)} \rho(A,B),\ \sup_{A\in F(g)} \inf_{B\in F(f)} \rho(A,B)\right\}.$$

It is not difficult to see [19] that $r(f,g)$ is a metric in $\mathcal{F}$, for which $r(f,0) = \|f\|$, but in general $r(f,g) \le \|f-g\|$. The latter shows that $\mathcal{F}$ metrized with Hausdorff metric is not a Banach space.

The Hausdorff distance, as the uniform distance, is sensitive to the change of the functions even in one point. For our purpose it is more convenient to use

the *Integral Hausdorff distance* defined through the *Hausdorff difference* between two functions [20].

**Definition 2.4.** The absolute value of the $\ominus$-*difference* between two functions $f, g \in \mathcal{F}$ in the point $x \in (0;0)$ is

$$|f(x) \ominus g(x)| = \max\{\inf_{(\xi,\eta)\in F(g)} \max[|x-\xi|, |f(x)-\eta|],$$

$$\inf_{(\xi,\eta)\in F(f)} \max[|x-\xi|, |g(x)-\eta|]\}.$$

Using the $\ominus$-difference we define the integral distance

$$R_p(f,g) = \left\{\int_0^1 [|f(x) \ominus g(x)|]^p dx\right\}^{1/p}, \quad 0 < p < \infty.$$

between two functions from $\mathcal{F}$.

The integral distance $R_p$ does not satisfy the triangle condition and is not a metric, but may be used to measure the closeness between two functions.

**Definition 2.5.** Let $f \in \mathcal{F}$ and

$$v((k;p), f) = \sup\{|f(x') - f(x'')| : \ x', x'' \in (k;p)\}.$$

We call

$$\tau(f; 2^{-k}) = \max\left\{v((k;p), f) : \ p = 0, 1, 2, \ldots, 2^k - 1\right\} \tag{2.2}$$

the *fractal modulus of continuity.*

**Definition 2.6** We call a fractal function *Hausdorff continuous* if

$$\lim_{s\to\infty} \tau(f; 2^{-s}) = 0.$$

The set of all Hausdorff continuous fractal functions is denoted by $\mathcal{HC}$.

**Definition 2.7.** For every $f \in \mathcal{F}$ we define

$$V_s(f) = \sum_{p=0}^{2^s-1} \left\{\overline{f}(p2^{-s}) - \underline{f}(p2^{-s}) + v((s;p), f)\right\},$$

$$\kappa_s(f) = s^{-1} \log_2 2^s (V_s(f) + 1) \tag{2.3}$$

and call the number

$$\kappa(f) = \overline{\lim_{s\to\infty}} \kappa_s(f)$$

*fractal dimension* of the function $f$.

This definition coincides with the usual definition of Hausdorff dimension [19] of the completed graph of the function $f$ and $1 \leq \kappa(f) \leq 2$, see [22] for the Hausdorff dimension of the completed graphs of multi-varied functions.

**Definition 2.8** A function $f \in \mathcal{F}$ is called a *pixel* function with *resolution* $s$ if $f$ is constant in every binary interval of rank $s$.

The set of all pixel functions with resolution $s$, denoted by $\mathcal{P}_s$, is a $2^s$ dimensional linear space.

**Definition 2.9** We shall use the linear operator $\Phi_s(f) = f^{<s>} : \mathcal{F} \to \mathcal{P}_s$, defined as follows:

$$\Phi_s(f;x) = f^{<s>}(x) = 2^s \int_{(s;p)} f(t)\,dt \quad \text{for} \quad x \in (s;p),\ p = 0,1,2,\ldots,2^s-1.$$

For every function $f \in \mathcal{F}$, $f^{<s>}$ is a pixel function with resolution $s$.

**Lemma 2.1** *For every $f \in \mathcal{F}$ the inequality*

$$\|f - \Phi_s(f)\| \leq \tau(f;2^{-s}) \tag{2.4}$$

*holds.*

Proof. From the definition of $\Phi_s(f)$ we have that for $x \in (s;p) \subset (0;0)$

$$\inf\{f(t) :\ t \in (s;p)\} \leq \Phi_s(f;x) \leq \sup\{f(t) :\ t \in (s;p)\}$$

and

$$|f(x) - \Phi_s(f;x)| \leq \sup\{|f(x') - f(x'')| :\ x', x'' \in (s;p)\} \leq \tau(f;2^{-s}).$$

From this () follows and the Lemma is proved. ∎

## 3. Orthonormal Extended Haar system

Let $\mathcal{F}_2$ be the space of the functions $\mathcal{F}$ with $L_2$ norm. We shall consider orthonormal systems $g_i \in \mathcal{F}_2$, $i = 0,1,2,\ldots$ and shall use the notation

$$g_n(f) = \int_0^1 f(x)g_n(x)\,dx;\ \ i = 0,1,2,\ldots$$

for the Fourier coefficients.

**Definition 3.1.** We define the pixel functions (see (2.1))

$$b_0(x) = 1,\quad b_n(x) = 2a_n(x) - 1;\quad n = 1,2,3,\ldots\ ,$$

$$c_n(x) = \begin{cases} b_n(x) & \text{for } x \in (1;0) \subset (0,1/2), \\ b_n(1-x) & \text{for } x \in (1;1) \subset (1/2,1), \\ 0 & \text{for } x \notin [0,1], \end{cases} \quad n = 2,3,4,\dots ,$$

$$c_{n,k,p}(x) = 2^{k/2} c_n(2^k x - p);$$

$$n = 2,3,4,\dots, \quad k = 0,1,2,\dots, \quad p = 0,1,2,\dots,2^k - 1,$$

and call the set of functions

$$b_n(x); \quad n = 0,1,2,\dots,$$

$$c_{n,k,p}(x); \quad n = 2,3,4,\dots \ , k = 0,1,2,\dots, \quad p = 0,1,2,\dots,2^k - 1,$$

defined on $(0;0)$, the *Extended Haar system.*

**Lemma 3.1.** *The Extended Haar system is orthonormal in* $\mathcal{F}_2$.

Proof. From the definition of $b_n(x)$ and $c_n(x)$ it follows that

$$b_n(x)^2 = (2a_n(x) - 1)^2 = 1 - 4a_n(x)(1 - a_n(x)) = 1,$$

as $a_n(x)$ is either 0 or 1. Then $c_n(x)^2 = 1$ and

$$\int_0^1 b_n(x)^2 \, dx = \int_0^1 c_n(x)^2 \, dx = 1.$$

In the same way

$$2^k \int_0^1 \left(c_n(2^k x - p)\right)^2 \, dx = 2^k \int_{(k;p)} \left(c_n(2^k x - p)\right)^2 \, dx$$

$$= 2^k 2^{-k} \int_0^1 (c_n(t))^2 \, dt = 1.$$

On the other hand it is immediately seen that

$$\int_0^1 b_m(x) b_n(x) \, dx = 0, \quad \text{for} \quad n \neq m,$$

$$\int_0^1 b_m(x) c_{n,k,p}(x) \, dx = \int_{(k;p)} b_m(x) c_n(2^k x - p) \, dx$$

$$= 2^{-k} \int_0^1 b_m(2^{-k}(t+p)) c_n(t) \, dt = 0,$$

for arbitrary $m$ and $n$; $k = 0,1,2,\dots, \quad p = 0,1,2,\dots,2^k - 1.$

We have also, for arbitrary $m$ and $n$

$$\int_0^1 c_m(2^k x - q)c_n(2^k x - p)\,dx = 0 \quad \text{if} \quad (k,p) \neq (l,q).$$

In fact:

1) For $l = k$ and $p \neq q$ the supports of $c_m(2^l x - q)$ and $c_n(2^k x - p)$ do not intersect.

2) For $l > k$ the supports of $c_m(2^l x - q)$ and $c_n(2^k x - p)$ intersect if $(l;q) \subset (k;p)$ or if $p = [q2^{k-l}]$, then

$$\int_0^1 c_m(2^l x - q)c_n(2^k x - [q2^{k-l}])\,dx = \int_{(l;p)} c_m(2^l x - q)c_n(2^k x - [q2^{k-l}])\,dx$$

$$= 2^{-l}\int_0^1 c_m(t)c_n(2^{k-l}(t + [p/2^{l-k}]) - [q2^{k-l}])\,dt = 2^{-l}\int_0^1 c_m(t)b_{n+k-l}(t)\,dt = 0$$

for arbitrary $m$ and $n$.

The case $m \neq n$ and $(k;p) = (l;q)$ is obvious.

That completes the proof. ∎

**Corollary 3.1.** *The functions*

$$b_n(x); \quad n = 0,1,2,\ldots,s\ ,$$

$$c_{n,k,p}(x); \quad n = 2,3,4,\ldots,s\ \ ,k = 0,1,2,\ldots,s-n\ \ ,p = 0,1,2,\ldots,2^k - 1,$$

*form the orthonormal Extended Haar basis in the set $\mathcal{P}_s$ of the pixel functions with resolution $s$.*

Since the number of all functions from the Extended Haar system with resolution $\leq s$ is $2^s$, from Lemma 3.1 and Corollary 3.1 it follows:

**Corollary 3.2.** *Every pixel function $f$ with resolution $s$ has the representation*

$$f(x) = \sum_{n=0}^{s} b_n(f)b_n(x) + \sum_{k=0}^{s-2}\sum_{n=2}^{s-k}\sum_{p=0}^{2^k-1} c_{n,k,p}(f)c_n(2^k x - p),$$

*where*

$$b_n(f) = \int_0^1 f(x)b_n(x)\,dx, \quad c_{n,k,p}(f) = \int_0^1 f(2^{-k}(x+p))c_n(x)\,dx,$$

*and the representation*

$$f(x) = \sum_{k=0}^{s-1} f_k(x), \tag{3.5}$$

*where*

$$f_0(x) = \sum_{n=0}^{s} b_n(f)b_n(x),$$

$$f_{k+1}(x) = \sum_{n=2}^{s-k} c_{n,k,p}(f)c_n(2^k x - p); \quad \text{for } x \in (k;p), \quad p = 0, 1, 2, \ldots, 2^k - 1.$$

The functions $f_0, f_1, f_2, \ldots, f_{s-2}$ in (3.5) are called *levels* of the function $f$.

**Theorem 3.1** *If a fractal function $f$ is Hausdorff continuous, then*

$$\lim_{s\to\infty} \left\| f(x) - \sum_{n=0}^{s} b_n(f)b_n(x) - \sum_{k=0}^{s-2}\sum_{n=2}^{s-k}\sum_{p=0}^{2^k-1} c_{n,k,p}(f)c_n(2^k x - p) \right\| = 0, \tag{3.6}$$

*where*

$$b_n(f) = \int_0^1 f(x)b_n(x)\,dx, \quad c_{n,k,p}(f) = \int_0^1 f(2^{-k}(x+p))c_n(x)\,dx.$$

Proof. According to Corollary 3.2,

$$f^{<s>}(x) = \sum_{n=0}^{s} b_n(f)b_n(x) + \sum_{k=0}^{s-2}\sum_{n=2}^{s-k}\sum_{p=0}^{2^k-1} c_{n,k,p}(f)c_n(2^k x - p),$$

then according to Lemma 2.1

$$\|f - f^{<s>}\| \le \tau(f; 2^{-s}).$$

Hence, the equality

$$\lim_{s\to\infty} \|f - f^{<s>}\| = 0$$

holds, which completes the proof. ∎

For illustrations in this paper we shall use a set of *source functions* depicted in Fig. 1 named according to Table 1.

All illustrations in this paper are based on the use of the pixel function $f^{(8)}$ for every function $f$ to be depicted.

To illustrate the representation (3.5) we present the completed graphs of the components of this representation for three of the source functions (see Fig. 2, Fig. 3, and Fig. 4).

The components $f_i$; $i = 5, 6, 7$ in the representation (3.5) of the function $f^{<8>}(x)$ for $f(x) = f_{(1,1)} = x^2$ in Fig. 2 are equal to zero.

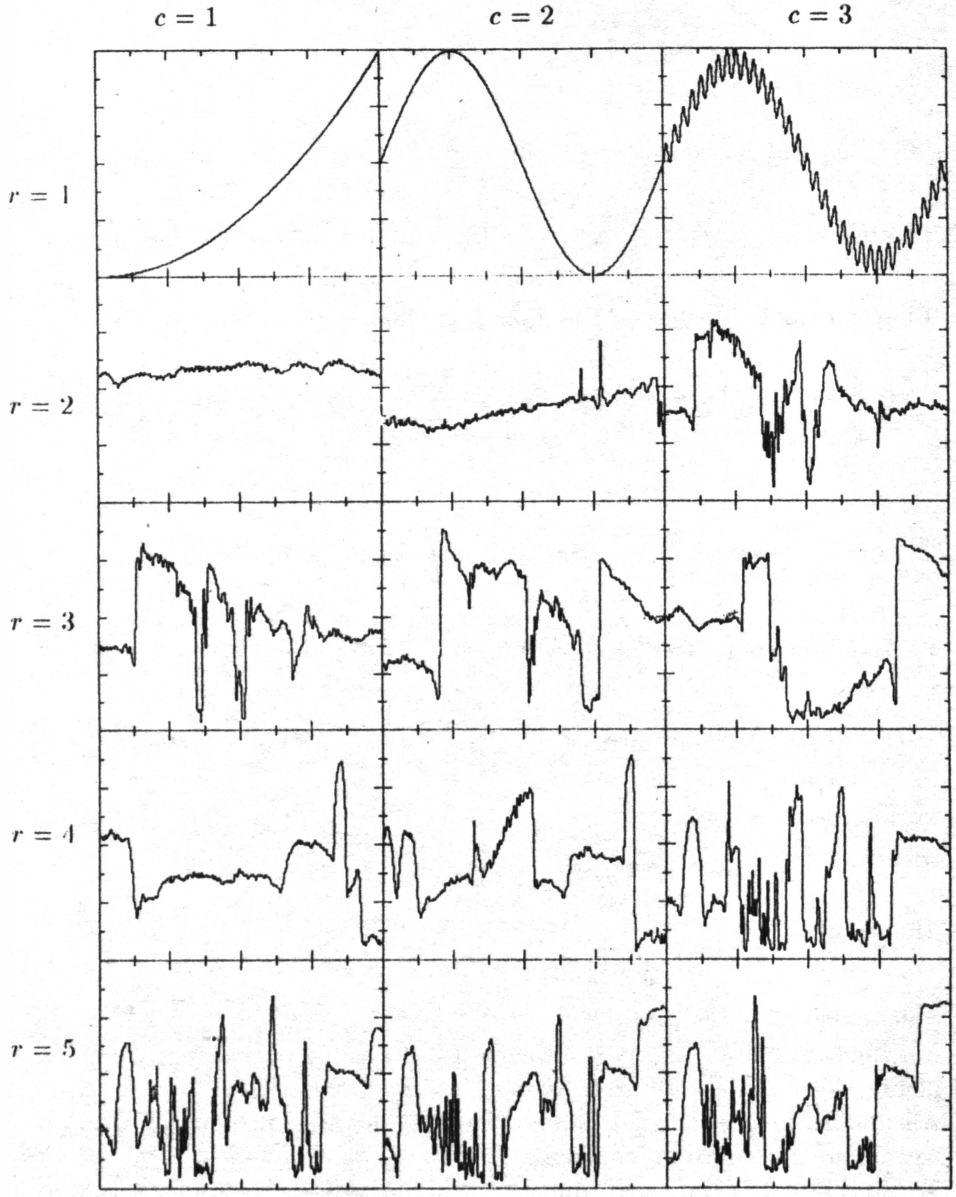


Figure 1: The completed graphs of the source functions $f_{(r,c)}$; $c = 1, 2, 3$; $r = 1, \ldots, 5$

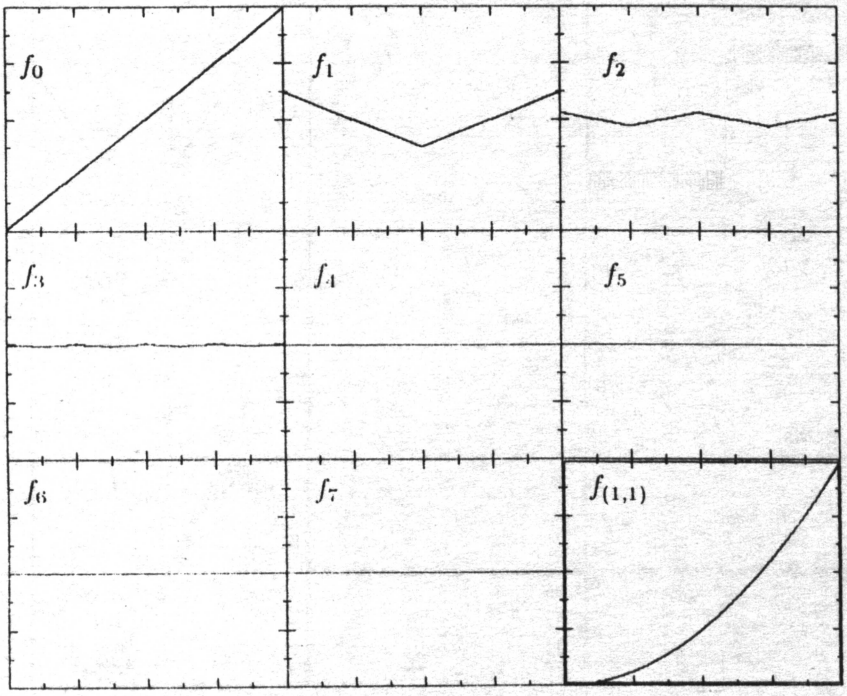


Figure 2: The levels of the function $f_{(1,1)}$, see representation (3.7).

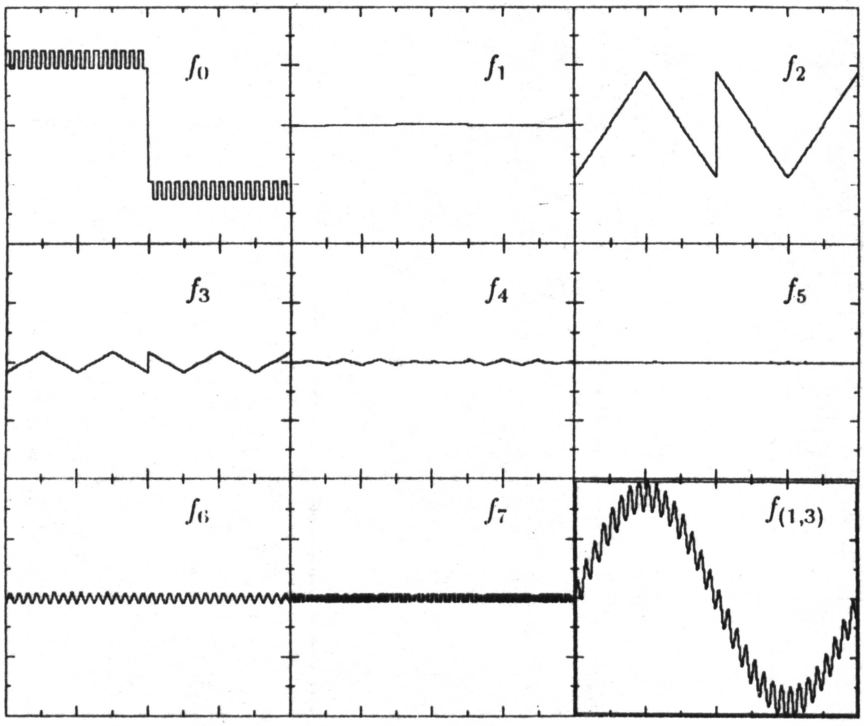


Figure 3: The levels of the function $f_{(1,3)}$.

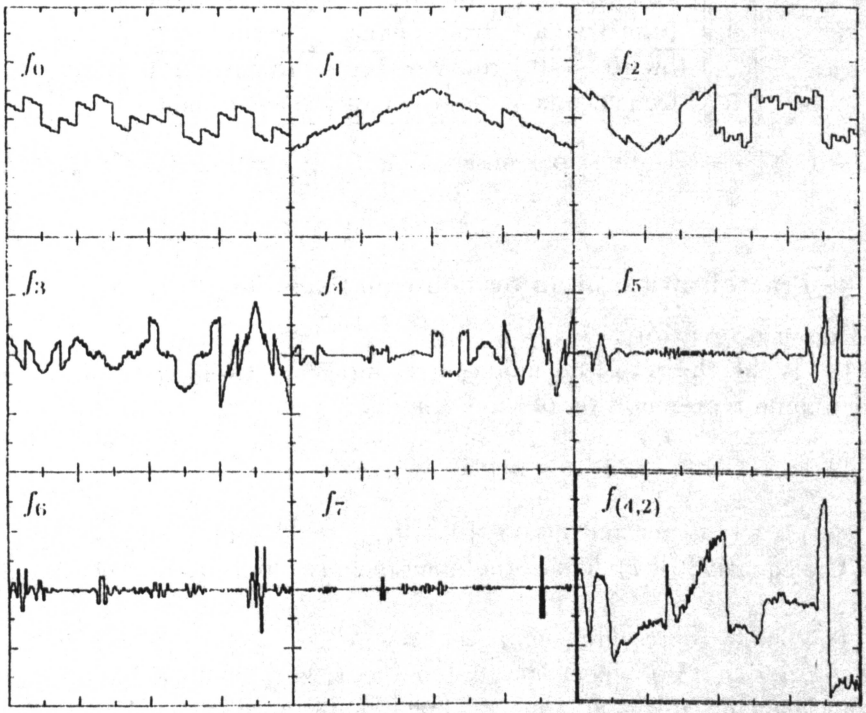


Figure 4: The levels of the function $f_{(4,2)}$.

| r | c=1 | c=2 | c=3 |
|---|---|---|---|
| 1 | $f(x) = x^2$ $x \in [0,1]$ | $f(x) = \sin x$ $x \in [0, 2\pi)$ | $f(x) = \frac{7}{8}\sin x$ $+\frac{1}{8}\sin 32x$ |
| 2 | col. No. 20 from Lenna | col. No. 30 from Lenna | col. No. 130 from Lenna |
| 3 | col. No. 140 from Lenna | col. No. 160 from Lenna | col. No. 176 from Lenna |
| 4 | row No. 20 from Lenna | row No. 30 from Lenna | row No. 130 from Lenna |
| 5 | row No. 140 from Lenna | row No. 160 from Lenna | row No. 176 from Lenna |

Table 1: The source functions description $f_{(r,c)}$; $c = 1, 2, 3$ , $r = 1, \ldots, 5$.

## 4. Fractalization of an orthonormal system

### 4.1. Binary operations

Let $\mathcal{N}$ be the set of all nonnegative integers. Every natural number $n$ has the unique representation of the form

$$n = 2^{\nu(n)} + \mu(n), \tag{4.7}$$

where $\nu(n)$ is an integer and $\mu(n) \in \{0, 1, 2, \ldots, 2^{\nu(n)} - 1\}$.

The equation (4.7) defines the functions $\nu(n)$ and $\mu(n)$ for every natural number $n$.

The binary representation of every $n \in \mathcal{N}$ is $n = n_0 + n_1 2^1 + n_2 2^2 + \ldots$ , or $n = (n_0, n_1, n_2, \ldots)$, where $n_i = 0, 1$; $i = 0, 1, 2, \ldots$ are the binary digits of $n$. In the following, if $n \in \mathcal{N}$, then $n_i$ shall denote the $i$th binary digit of $n$.

If $n_i$ is a binary digit, then by $\overline{n}_i$ is denoted the inverse value of this digit, i.e., $\overline{0} = 1$ and $\overline{1} = 0$.

For $i \in \mathcal{N}$ denote by $n(\overline{i})$ the number produced from the number $n$ by reversing the $i$-th digit of $n$. For example

$$11(\overline{4}) = (1, 1, 0, 1, 0, 0, 0, \ldots)(\overline{4}) = (1, 1, 0, 1, 1, 0, 0, \ldots) = 27.$$

For the binary digits we use the addition (mod 2), denoted by " $\oplus$ ", or the binary addition:

$$0 \oplus 0 = 1 \oplus 1 = 0, \quad 0 \oplus 1 = 1 \oplus 0 = 1.$$

We define the *binary addition* " $\oplus$ " in $\mathcal{N}$ :

$$m \oplus n = (m_0 \oplus n_0, m_1 \oplus n_1, m_2 \oplus n_2, \dots ).$$

For example,

$$5 \oplus 9 = (1,0,1,0,0,0,\dots) \oplus (1,0,0,1,0,0,0,\dots) = (0,0,1,1,0,0,0,\dots) = 12.$$

**Lemma 4.1.** *For every $n, p, q \in \mathcal{N}$ from $n \oplus p = n \oplus q$ it follows that $p = q$, or that in the set*

$$n \oplus \mathcal{N} = \{n \oplus 0, n \oplus 1, n \oplus 2, \dots\}$$

*all members are different and that $n \oplus \mathcal{N} = \mathcal{N}$.*

Proof.

$$n \oplus p = (n_0 \oplus p_0, n_1 \oplus p_1, \dots) = (n_0 \oplus q_0, n_1 \oplus q_1, \dots) = n \oplus q,$$

hence

$$n_i \oplus p_i = n_i \oplus q_i; \quad i = 0, 1, 2, \dots,$$

or $p_i = q_i; \quad i = 0, 1, 2, \dots$ .

We define the *binary scalar product* of two integers $m, n \in \mathcal{N}$, two binary codes, as follows:

$$\langle n, m \rangle = \sum_{i=0}^{\infty} n_i m_i < \infty.$$

For example $\langle 5, 9 \rangle = 1, \ \langle 6, 7 \rangle = 2$.

**Lemma 4.2.** *If $m, n, k \in \mathcal{N}$, $m \neq n$ and the equation*

$$(m_0 \oplus x_0 + n_0 \oplus x_0, m_1 \oplus x_1 + n_1 \oplus x_1, m_2 \oplus x_2 + n_2 \oplus x_2, \dots) = (k_0, k_1, k_2, \dots) \tag{4.8}$$

*has a solution $x' = (x'_0, x'_1, x'_2, \dots) \in \mathcal{N}$, then (4.8) has also another solution $x'' \in \mathcal{N}$ such that*

$$(-1)^{\langle m, x'' \rangle + \langle n, x'' \rangle} = -(-1)^{\langle m, x' \rangle + \langle n, x' \rangle}. \tag{4.9}$$

Proof. As $m \neq n$, there exists an index $s$ such that $m_s \neq n_s$. Then the other solution of (4.8) with the property (4.9) is $x'' = x'(\overline{s})$ as

$$m_s \oplus x'_s + n_s \oplus x'_s = 1 = m_s \oplus \overline{x'_s} + m_s \oplus \overline{x'_s}.$$

### 4.2. Orthogonal sequences

For every number $\lambda$ and for every nonnegative integer $n$ we define the sequence $\{\sigma_{n,i}(\lambda)\}_{i=1}^{\infty}$ as follows:

$$\sigma_{n,i}(\lambda) = (-1)^{\langle n,i\rangle}\lambda^{n\oplus i} \quad \text{for} \quad i = 0,1,2,\dots \,. \tag{4.10}$$

The first 8 sequences are:

$$\begin{aligned}
\sigma_{0,i}(\lambda) &= 1, \quad \lambda, \quad \lambda^2, \quad \lambda^3, \quad \lambda^4, \quad \lambda^5, \quad \lambda^6, \quad \lambda^7, \quad \dots \\
\sigma_{1,i}(\lambda) &= \lambda, \quad -1, \quad \lambda^3, \quad -\lambda^2, \quad \lambda^5, \quad -\lambda^4, \quad \lambda^7, \quad -\lambda^6, \quad \dots \\
\sigma_{2,i}(\lambda) &= \lambda^2, \quad \lambda^3, \quad -1, \quad -\lambda, \quad \lambda^6, \quad \lambda^7, \quad -\lambda^4, \quad -\lambda^5, \quad \dots \\
\sigma_{3,i}(\lambda) &= \lambda^3, \quad -\lambda^2, \quad -\lambda, \quad 1, \quad \lambda^7, \quad -\lambda^6, \quad -\lambda^5, \quad \lambda^4, \quad \dots \\
\sigma_{4,i}(\lambda) &= \lambda^4, \quad \lambda^5, \quad \lambda^6, \quad \lambda^7, \quad -1, \quad -\lambda, \quad -\lambda^2, \quad -\lambda^3, \quad \dots \\
\sigma_{5,i}(\lambda) &= \lambda^5, \quad -\lambda^4, \quad \lambda^7, \quad -\lambda^6, \quad -\lambda, \quad 1, \quad -\lambda^3, \quad \lambda^2, \quad \dots \\
\sigma_{6,i}(\lambda) &= \lambda^6, \quad \lambda^7, \quad -\lambda^4, \quad -\lambda^5, \quad -\lambda^2, \quad -\lambda^3, \quad 1, \quad \lambda, \quad \dots \\
\sigma_{7,i}(\lambda) &= \lambda^7, \quad -\lambda^6, \quad -\lambda^5, \quad \lambda^4, \quad -\lambda^3, \quad \lambda^2, \quad \lambda, \quad -1, \quad \dots
\end{aligned}$$

From the definition (4.10) it follows that

$$\sigma_{n,i+q}(\lambda) = \lambda^q \sigma_{n,i}(\lambda) \quad \text{for} \quad q = 2^{\nu(n)+1}. \tag{4.11}$$

**Lemma 4.3.** *For* $|\lambda| < 1$

$$\sum_{i=0}^{\infty} \sigma_{m,i}(\lambda)\sigma_{n,i}(\lambda) = \begin{cases} \frac{1}{1-\lambda^2} & \text{for} \quad m = n, \\ 0 & \text{for} \quad m \neq n. \end{cases}$$

Proof. For $m = n$, from Lemma we have that

$$\sum_{i=0}^{\infty} \sigma_{n,i}(\lambda)\sigma_{n,i}(\lambda) = \sum_{i=0}^{\infty} \lambda^{2i} = \frac{1}{1-\lambda^2}.$$

For $m \neq n$, from Lemma we have that

$$\sum_{i=0}^{\infty} \sigma_{m,i}(\lambda)\sigma_{n,i}(\lambda) = 0 \tag{4.12}$$

since to every member of the sum (4.12) there corresponds an opposite member.

**Definition 4.1** Let $g_i(x)$; $i = 0, 1, 2, \ldots$ be an orthonormal system in $\mathcal{F}_2$. The system

$$g_n(\lambda; x) = \sqrt{1-\lambda^2} \sum_{i=0}^{\infty} \sigma_{n,i}(\lambda) g_i(x), ; \quad n = 0, 1, 2, \ldots \tag{4.13}$$

is the *fractalized* system $\{g_i(x)\}_{i=1}^{\infty}$ with **fractalization parameter** $\lambda$.

**Lemma 4.4.** *The system (4.13) is orthonormal.*

Proof. From the Definition 4.1 and Lemma 4.3, we have

$$\int_0^1 g_m(\lambda; x) g_n(\lambda; x)\, dx = (1-\lambda^2) \sum_{i=0}^{\infty} \sigma_{m,i}(\lambda)\sigma_{n,i}(\lambda) = \begin{cases} 1 & \text{for } m = n, \\ 0 & \text{for } m \neq n. \end{cases}$$

That completes the proof. ∎

**Definition 4.2.** We say that the orthogonal system $g_n(x)$; $n = 1, 2, 3, \ldots$ is *fractalizable*, if for every number $\alpha \in [0, 1)$ there exists a number $\lambda \in (-1, 1)$ such that every function $g_n(\lambda; x)$ from ( ) has a fractal dimension $\kappa(g_n(\lambda; .)) = 1 + \alpha$.

It is easy to see that the orthogonal system $g_n(t) = \cos(2\pi n t)$; $n = 0, 1, 2, \ldots$ is not fractalizable, but its subsystem $g_n^*(t) = \cos(2^n \pi t)$; $n = 0, 1, 2, \ldots$ is fractalizable. With the first step of fractalizing of the system $\{\cos(2^n \pi t)\}_{n=1}^{\infty}$ we produce the celebrated Weierstrass function [10]

$$W_\alpha(t) = \sum_{i=1}^{\infty} \lambda^i \cos(2^i \pi t), \quad 1/2 \leq \lambda < 1$$

with fractal dimension $1 + \alpha$ [16], where $\alpha = 1 + \log_2 \lambda$.

**Definition 4.3.** We extend the definition of a fractalizable system calling an orthonormal system *fractalizable* if all its functions, except the first, may be divided into a series of fractalizable systems.

## 5. Fractalization of the Extended Haar system

We shall show that the Extended Haar system is fractalizable if it is divided in the following series of orthonormal subsystems, starting after the first function $b_0(x) = 1$ of this system:

$$b_n(x) = 2a_n(x) - 1; \quad n = 1, 2, 3, \ldots \tag{5.14}$$

and

$$c_{n,k,p}(x) = 2^{k/2} c_n(2^k x - p); \quad n = 2, 3, 4, \ldots \quad , \tag{5.15}$$

where

$$k = 0, 1, 2, \ldots, \quad p = 0, 1, 2, \ldots, 2^k - 1$$

and

$$c_n(x) = \begin{cases} b_n(x) & \text{for} \quad x \in (1;0) \subset (0,1/2), \\ b_n(1-x) & \text{for} \quad x \in (1;1) \subset (1/2,1), \\ 0 & \text{for} \quad x \notin [0,1], \end{cases} \quad n = 2, 3, 4, \ldots \ ,$$

**Definition 5.1.** We fractalize the Extended Haar system by fractalizing the subsystems (5.14),(5.15) and denote

$$\psi_n(\lambda; x) = \sqrt{1-\lambda^2} \sum_{i=0}^{\infty} \sigma_{n,i}(\lambda) b_{i+1}(x); \quad n = 0, 1, 2, \ldots \ , \tag{5.16}$$

and

$$\phi_{n,k,p}(\lambda; x) = \sqrt{1-\lambda^2} \sum_{i=0}^{\infty} \sigma_{n,i}(\lambda) c_{i+2,k,p}(x); \quad n = 0, 1, 2, \ldots \ , \tag{5.17}$$

where $k = 0, 1, 2, \ldots, \quad p = 0, 1, 2, \ldots, 2^k - 1$.

In Fig 5 the completed graphs of the basic functions $\psi_n(\lambda; x)$ are depicted for $n = 0, 1, 2, 3$ in the columns and for $\lambda = -0.75, -0.50, -0.25, 0.25, 0.50, 0.75$ in the rows.

We shall prove later that the functions (5.16) and (5.17) are Hausdorff continuous, see Corollary 5.1.

**Lemma 5.1** *Every function from (5.16) and (5.17) has a fractal dimension 1 for* $0 \le |\lambda| \le \frac{1}{2}$ *and a fractal dimension* $1+\alpha$ *for* $|\lambda| = 2^{\alpha-1}$; $\frac{1}{2} \le |\lambda| < 1$.

Proof. We shall prove the Lemma only for the functions (5.16), since the proof for the rest of the functions is the same.

According to Definition 2.7, we have to estimate, for a fixed $n$, the value of

$$V_s(\psi_n(\lambda; .)) = \sum_{p=0}^{2^s-1} \left\{ \overline{\psi}_n(\lambda; p2^{-s}) - \underline{\psi}_n(\lambda; p2^{-s}) \right\} + \sum_{p=0}^{2^s-1} v((s;p), \psi_n(\lambda; .)) = A + B.$$

From the definition of $b_i(x)$, for $x = (2p+1)2^{-k-1}$, we have

$$b_i(x+0) = b_i(x-0) \quad \text{if} \quad i \le k,$$

$$b_i(x+0) = -b_i(x-0) = -1 \quad \text{if} \quad i > k+1,$$

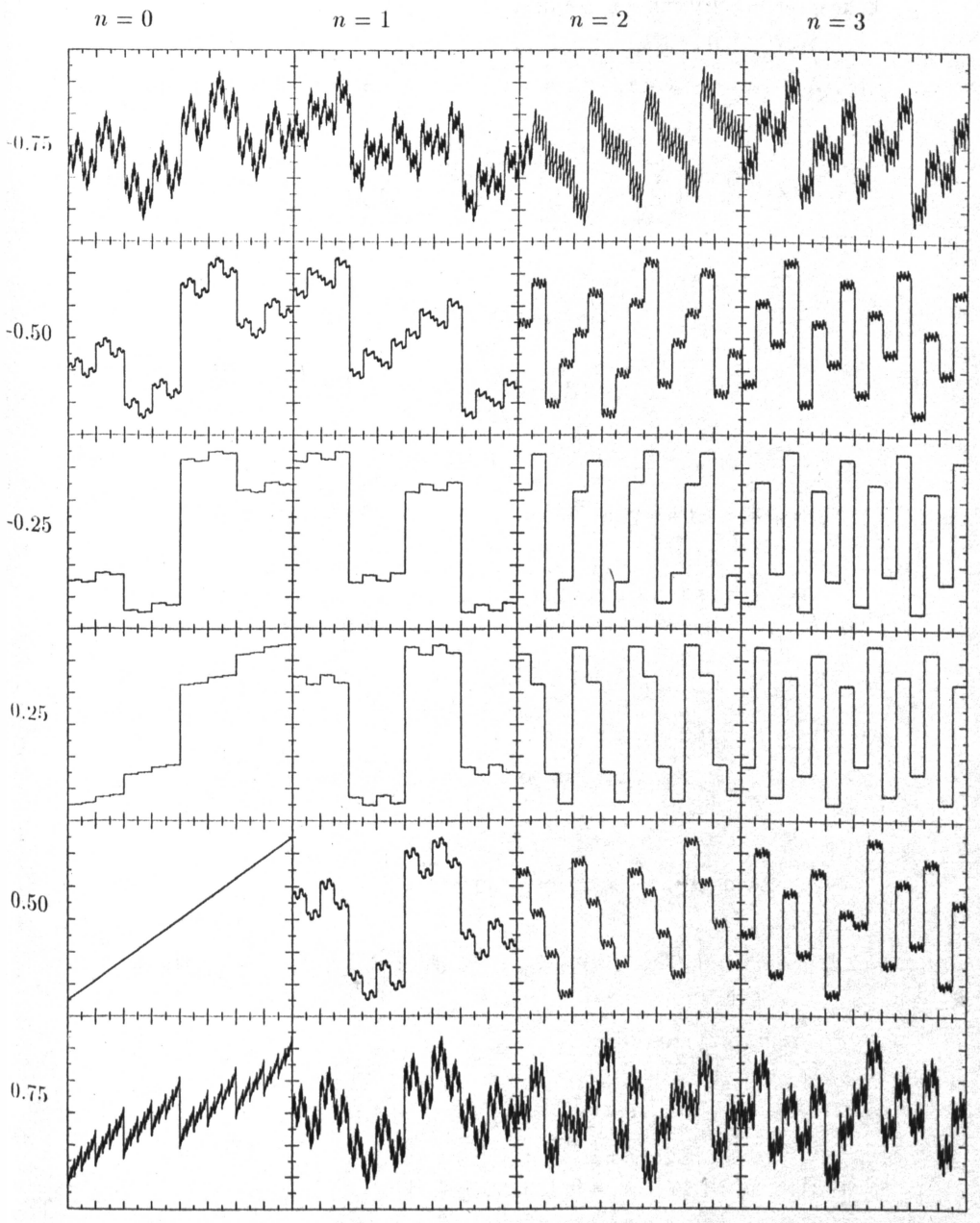


Figure 5: Basic functions $\psi_n(\lambda; x)$; $n = 0, 1, 2, 3$; $\lambda = -0.75, -0.50, -0.25, 0.25, 0.50, 0.75$ .

hence, setting $2^{\nu(n)+1} = q$, we have

$$|\psi_n(\lambda; x+0) - \psi_n(\lambda; x-0)| = \sqrt{1-\lambda^2}\left|\sum_{i=k+1}^{\infty} \sigma_{n,i}(\lambda)\{b_i(x+0) - b_i(x-0)\}\right|$$

$$= 2\sqrt{1-\lambda^2}\left|\sum_{i=k+1}^{\infty} \sigma_{n,i}(\lambda)\right| = 2\sqrt{1-\lambda^2}\left|\sum_{i=0}^{\infty}(-1)^{\langle n,k+i+1\rangle}\lambda^{n\oplus(k+i+1)}\right|$$

$$= 2\sqrt{1-\lambda^2}\left|\sum_{s=0}^{\infty}\sum_{j=0}^{q-1}(-1)^{\langle n,k+sq+j+1\rangle}\lambda^{n\oplus(k+sq+j+1)}\right|$$

$$= 2\sqrt{1-\lambda^2}\left|\sum_{s=0}^{\infty}\lambda^{sq}\sum_{j=0}^{q-1}(-1)^{\langle n,k+j+1\rangle}\lambda^{n\oplus(k+j+1)}\right|,$$

or

$$|\psi_n(\lambda; x+0) - \psi_n(\lambda; x-0)| = \frac{2\sqrt{1-\lambda^2}}{1-\lambda^q}\left|\sum_{j=0}^{q-1}(-1)^{\langle n,k+j+1\rangle}\lambda^{n\oplus(k+j+1)}\right|. \tag{5.18}$$

Let $k = lq + i$, $0 \le i \le q-1$. Then $\langle n, k+j+1\rangle = \langle n, i+j+1\rangle$ and $(n \oplus (k+j+1)) - k = (n \oplus (i+j+1)) - i$, and from (5.18) we have

$$|\psi_n(\lambda; x+0) - \psi_n(\lambda; x-0)| = |\lambda|^k A_{n,i}, \tag{5.19}$$

where

$$A_{n,i} = \frac{2\sqrt{1-\lambda^2}}{1-\lambda^q}\left|\sum_{j=0}^{q-1}(-1)^{\langle n,i+j+1\rangle}\lambda^{(n\oplus(i+j+1))-i}\right|. \tag{5.20}$$

Consequently, for $x = (2p+1)2^{-k-1}$,

$$\sum_{p=0}^{2^k-1}|\psi_n(\lambda; x+0) - \psi_n(\lambda; x-0)| = \sum_{p=0}^{2^k-1}|\lambda|^k A_{n,i} = (2|\lambda|)^k A_{n,i}. \tag{5.21}$$

From (5.21) we have

$$A = \sum_{k=1}^{s} A_{n,i(k)}(2|\lambda|)^k = A_s(2|\lambda|)^s, \tag{5.22}$$

where $A_s \le \max\{A_{n,i} : \ i = 0, 1, 2, \ldots, q-1\}$.

In the same way we obtain

$$B = B_s(2|\lambda|)^s. \tag{5.23}$$

From (5.22) and (5.23), according to Definition 2.7, we have

$$V_s(\psi_n(\lambda;.)) = (A_s + B_s)(2|\lambda|)^s = C_s(2|\lambda|)^s,$$

hence

$$\kappa(\psi_n(\lambda;.)) = \overline{\lim_{s\to\infty}} s^{-1}\log_2 2^s\,(C_s(2|\lambda|)^s + 1)$$

and

$$\kappa(\psi_n(\lambda;.)) = \begin{cases} 1 & \text{for } 0 \le |\lambda| \le \frac{1}{2}, \\ 1+\alpha & \text{for } \frac{1}{2} \le |\lambda| = 2^{\alpha-1} < 1, \end{cases}$$

which completes the proof. ∎

From Lemma 5.1 there follows:

**Theorem 5.1.** *The Extended Haar system is fractalizable.*

Remark 5.1. Every subsystem of the Extended Haar system may be fractalized with different fractalization parameter $\lambda$.

### 5.1. IFS and fractalization

**Definition 5.2.** Let $k$ be a natural number, $B_k = \{b_0, b_1, b_2, \ldots, b_{2^k-1}\}$ be a $2^k$-dimensional vector and let $\lambda \in (-1, 1)$ be a number. The iterative equation

$$f(x) = \lambda f(2^k x - p) + b_p \quad \text{for} \quad x \in (k;p);\ p = 0, 1, 2, \ldots, 2^k - 1 \tag{5.24}$$

is equivalent to a IFS with $2^k$ mappings.

We call a *simple* IFS, or SIFS of rank $k$, the IFS equivalent to (5.24) . The fixed point of (5.24) is denoted by $f_{B_k}(\lambda; x)$.

**Lemma 5.2** *The fixed point $\phi = f_{B_k}(\lambda;.)$ of the IFS () is Hausdorff continuous, or $\phi \in \mathcal{HC}$.*

Proof. From () we have

$$\tau(\phi; 2^{-k}) \le |\lambda|\tau(\phi; 1)$$

and

$$\tau(\phi; 2^{-sk}) \le |\lambda|^s\tau(\phi; 1),$$

which completes the proof as $|\lambda| < 1$. ∎

It is easy to prove that the function $f_{B_k}(\lambda;.)$ is Lebesgue integrable in the interval $[0,1]$ for every vector $B_k$ and every number $\lambda \in (-1,1)$.

**Lemma 5.3.** *Let $f_{B_k}(\lambda;.)$ and $f_{C_k}(\mu;.)$ be the fixed points of () for the two vectors $B_k$, $C_k$ and the two numbers $\lambda$, $\mu$. If $\sum_{p=0}^{2^k-1} b_p = \sum_{p=0}^{2^k-1} c_p = 0$ and the vectors $B_k$, $C_k$ are orthogonal, i.e., $\sum_{p=0}^{2^k-1} b_k c_k = 0$, then the functions $f_{B_k}(\lambda;.)$, $f_{C_k}(\mu;.)$ are orthogonal, i.e.,*

$$\int_0^1 f_{B_k}(\lambda;x) f_{C_k}(\mu;x)\,dx = 0.$$

Proof. From (5.24) we have

$$I = \int_0^1 f_{B_k}(\lambda;x) f_{C_k}(\mu;x)\,dx =$$

$$\lambda\mu \sum_{p=0}^{2^k-1} \int_{(k;p)} f_{B_k}(\lambda;2^k x - p) f_{C_k}(\mu;2^k x - p)\,dx$$

$$+\lambda \sum_{p=0}^{2^k-1} b_p \int_{(k;p)} f_{C_k}(\mu;2^k x - p)\,dx + \mu \sum_{p=0}^{2^k-1} c_p \int_{(k;p)} f_{B_k}(\lambda;2^k x - p)\,dx$$

$$+ \sum_{p=0}^{2^k-1} b_k c_k = \lambda\mu 2^{-k} \sum_{p=0}^{2^k-1} \int_0^1 f_{B_k}(\lambda;t) f_{C_k}(\mu;t)\,dt$$

$$+\lambda 2^{-k} \int_0^1 f_{C_k}(\mu;t)\,dt \sum_{p=0}^{2^k-1} b_p + \mu 2^{-k} \int_0^1 f_{B_k}(\lambda;t)\,dt \sum_{p=0}^{2^k-1} c_p + \sum_{p=0}^{2^k-1} b_k c_k$$

$$= \lambda\mu \int_0^1 f_{B_k}(\lambda;t) f_{C_k}(\mu;t)\,dt,$$

or

$$(1 - \lambda\mu) I = 0,$$

hence $I = 0$, as $1 - \lambda\mu \neq 0$. ∎

**Lemma 5.4** *Every function $\psi_k(\lambda;x)$ is a fixed point of a SIFS of rank $q = 2^{\nu(k)+1}$ and every function $\phi_k(\lambda;x)$ is a fixed point of a SIFS of rank $q = 2^{\nu(k)+2}$.*

Proof. From (5.16) and (4.11) we have for $q = 2^{\nu(k)+1}$ that

$$\psi_k(\lambda;x) = \sqrt{1-\lambda^2} \sum_{i=1}^{\infty} \sigma_{k,i}(\lambda) b_i(x) \tag{5.25}$$

$$= \sqrt{1-\lambda^2}\sum_{i=0}^{q-1}\sigma_{k,i}(\lambda)b_i(x) + \sqrt{1-\lambda^2}\lambda^q\sum_{i=0}^{\infty}\sigma_{k,i}(\lambda)b_{i+q}(x).$$

For $x \in (q;p)$ and $i = 0,1,2,\ldots,q-1$, the functions $b_i(x) = b_{p,i}$ are constants, moreover

$$b_{i+q}(x) = b_i(qx-p); \quad i = 0,1,2,\ldots \quad . \tag{5.26}$$

From (5.25) and (5.26) we get

$$\psi_k(\lambda;x) = \lambda^q\psi_k(\lambda;2^qx-p) + b_p, \quad \text{for} \quad x \in (q;p),$$

where

$$b_p = \sqrt{1-\lambda^2}\sum_{i=0}^{q-1}\sigma_{k,i}(\lambda)b_{p,i}.$$

In the same way we prove that, for $q = 2^{2^{\nu(n)}+2}$

$$\phi_k(\lambda;x) = \lambda^q\phi_k(\lambda;2^qx-p) + c_p, \quad \text{for} \quad x \in (q;p),$$

where

$$c_p = \sqrt{1-\lambda^2}\sum_{i=0}^{q-1}\sigma_{k,i}(\lambda)c_{p,i}.$$

From Lemma 5.4 and Lemma 5.2 it follows

**Corollary 5.1.** *All functions (5.16) and (5.17) are Hausdorff continuous.*

## 6. Compression of pixel functions

The digital representations of signals and images are in fact pixel functions of one or two variables. In this section we present computer experiments for compression of pixel functions using their representation by different transform coding and compare the quality of the recovery of these functions from the compressed data. For this calculations we use pixel functions $f \in \mathcal{P}_8$ (with resolution 8) and the values of the pixel functions are given with 8 bits (one byte). Every pixel function is defined exactly by $2^{11} = 2048$ bits.

If $G = \{l_i\}_{i=0}^{2^s-1}$ is the orthonormal basis

$$l_i(x) = \begin{cases} 2^s & \text{for} \quad x \in (s;i), \\ 0 & \text{for} \quad x \notin (s;i), \end{cases} \quad i = 0,1,2,\ldots,2^s-1$$

in $\mathcal{P}_s$, then every pixel function $f$ with resolution $s$ is represented exactly in the form

$$f(x) = \sum_{i=0}^{2^s-1} l_i(f) l_i(x),$$

where

$$l_i(f) = \int_0^1 f(x) l_i(x)\, dx$$

are the Fourier coefficients of $f$ for the basis $G$.

Every other orthonormal basis $G^*$ in $\mathcal{P}_s$ transforms the $N = 2^s$ dimensional vector, formed by the values of a pixel function $f \in \mathcal{P}_s$, in a $N = 2^s$ dimensional vector formed by the Fourier coefficients of this function for the basis $G^*$.

The technique of the *compression* consists of the following. We choose an a priori compression factor $c^* > 1$ and take $N/c^*$ number of the Fourier coefficients for a function $f$. It is natural to take the coefficients with biggest absolute values. Then we recover the function from these $N/c^*$ coefficients, taking the rest equal to zero. The quality of the recovery of a given function from the compressed coefficients with regard to different transform coding will be different. In addition, we may measure the quality of the recovery in different ways.

We have also the a posteriori compression factor $c$ giving the real compression. Let all the values of a pixel function be recorded by $M$ bits. If the compressed coefficients of this function may be recorded by $M'$ bits then the a posteriori compression factor is $c = M/M'$. Usually $c > c^*$ as we may use additional conventional methods for data compression as quantization and entropy coding. The a posteriori compression factor $c$ is more important for the practice of compression. In the following, the compression factor is always the a priori compression factor $c^*$.

In our computational experiment we use the following orthonormal bases in $\mathcal{P}_8$:

$H$ - the classical Haar basis,

$EH$ - the Extended Haar basis, and

$F(\lambda)$ - the fractalized Extended Haar basis with fractalization parameter $\lambda$. ($EH = F(0)$).

To "fractalize" the Extended Haar basis in $\mathcal{P}_8$ we have to use subsystems with 8, 7, 6, 5, 4, 3, 2 and 1 elements. For the subsystems with 7, 6, 5 and 3 elements the "fractalizing" procedure do not produce systems of orthogonal vectors. In this cases we orthogonalize the produced systems by Gram - Schmidt algorithm.

| | H | EH | F(.25) | F(.50) | F(.75) | F(-.75) | F(-.50) | F(-.25) |
|---|---|---|---|---|---|---|---|---|
| $l_1$ | .00830 | .00191 | .00172 | .00114 | .00186 | .00246 | .00127 | .00198 |
| $l_2$ | .01001 | .00279 | .00266 | .00211 | .00278 | .00337 | .00222 | .00295 |
| $l_\infty$ | .01953 | .00781 | .00781 | .00391 | .00781 | .00781 | .00391 | .00781 |
| $R_1$ | .00427 | .00186 | .00168 | .00114 | .00179 | .00223 | .00127 | .00185 |
| $R_2$ | .00483 | .00270 | .00256 | .00211 | .00264 | .00295 | .00222 | .00269 |
| $r$ | .01953 | .00391 | .00391 | .00391 | .00391 | .00391 | .00391 | .00391 |

Table 2: Approximation error for 4 times compression of the function $f_{(1,2)}$.

Remark 6.1. In this paper we use fractal bases with only one fractalization parameter. It is possible to use a different fractalization parameter for every one of the subsystems (5.14),(5.15), see Remark 5.1. But the use of a substantial number of fractalization parameters increases the volume of the data. Optimizing the number of the different fractalization parameters is an attractive but very difficult problem.

For measuring the quality of the reproduction we use the distances:

$l_1$ - $l_1(f,g) = 2^{-s}\sum_{i=0}^{2^s-1}|f((2i+1)2^{-s} - g((2i+1)2^{-s})|$,

$l_2$ - $l_2(f,g) = \left\{2^{-s}\sum_{i=0}^{2^s-1}(f((2i+1)2^{-s}) - g((2i+1)2^{-s}))^2\right\}^{1/2}$,

$l_\infty$ - the uniform distance,

$R_1$ - the Integral Hausdorff distance for $p = 1$,

$R_2$ - the Integral Hausdorff distance for $p = 2$, and

$r$ - the Hausdorff distance.

In Fig. 6. the recovery of a smooth source function $f_{(1,2)}$ is depicted after compression of different transform coding: Haar, Extended Haar and tree Fractal transform coding for three different values of the fractalization parameter.

In the left column the compression factor is 4, in the right column the compression factor is 16.

The recovery with Extended Haar is better then with Haar. The best is the recovery from Fractal basis with fractalization parameter $\lambda = \frac{1}{2}$ which corresponds to a fractal dimension $\kappa = 1$ of the basic functions , equal to the fractal dimension of the approximated function.

The quantitative measures for the quality of the recovery of the smooth source function $f_{(1,2)}$ in Fig. 6. are given in Table 2. and Table 3. From these tables it is seen that the smallest error for all distances is for the fractal transform coding $F(.50)$. The numerical data in this tables concur with the visual impression from Fig. 6.

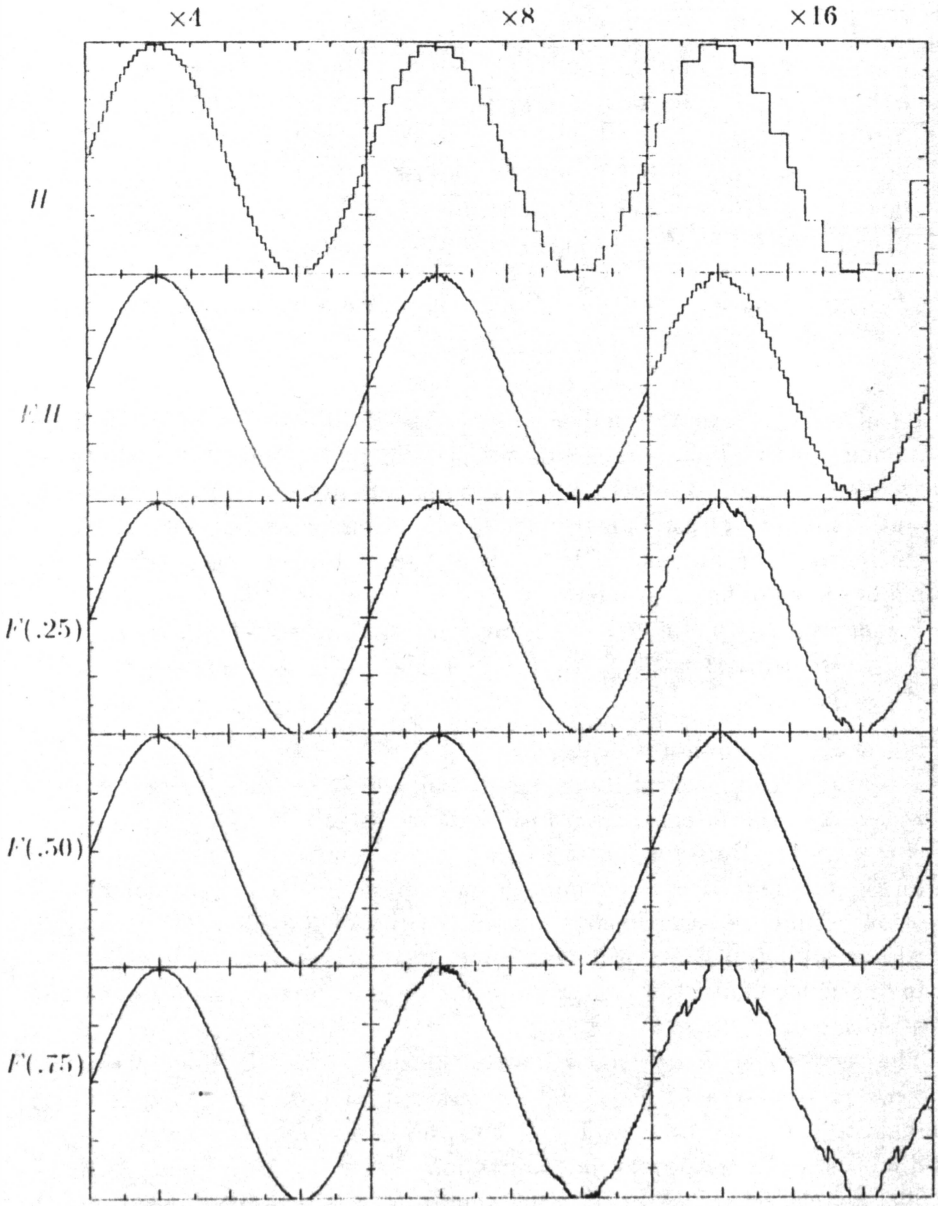


Figure 6: Recovery of the function $f_{(1,2)}$ after compression.

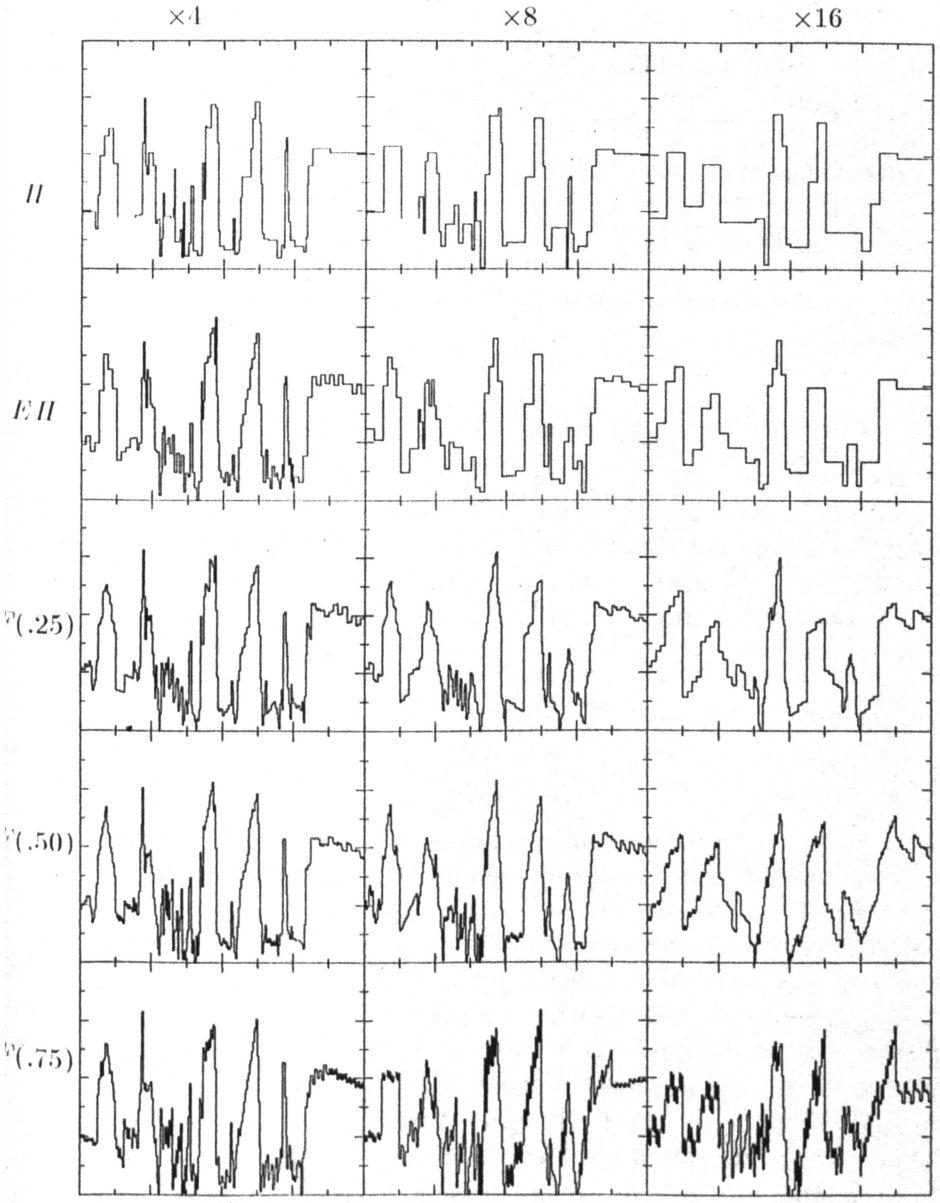


Figure 7: Recovery of the function $f_{(4,3)}$ after compression.

| | H | EH | F(.25) | F(.50) | F(.75) | F(-.75) | F(-.50) | F(-.25) |
|---|---|---|---|---|---|---|---|---|
| $l_1$ | .02853 | .01361 | .01205 | .00674 | .03409 | .04114 | .01462 | .01965 |
| $l_2$ | .03632 | .01710 | .01473 | .00863 | .04238 | .05015 | .01845 | .02392 |
| $l_\infty$ | .09375 | .05078 | .03906 | .02344 | .08203 | .11719 | .04688 | .06250 |
| $R_1$ | .01398 | .00749 | .00636 | .00453 | .01675 | .01736 | .00702 | .01105 |
| $R_2$ | .01720 | .01013 | .00823 | .00601 | .02330 | .02516 | .00965 | .01560 |
| $r$ | .08984 | .04688 | .03125 | .02344 | .07813 | .10156 | .04688 | .06250 |

Table 3: Approximation error for 16 times compression of the function $f_{(1,2)}$.

| | H | EH | F(.25) | F(.50) | F(.75) | F(-.75) | F(-.50) | F(-.25) |
|---|---|---|---|---|---|---|---|---|
| $l_1$ | .02507 | .03737 | .03185 | .02489 | .03447 | .04155 | .03340 | .03770 |
| $l_2$ | .03355 | .05062 | .04225 | .03339 | .04684 | .05490 | .04605 | .04957 |
| $l_\infty$ | .15625 | .20703 | .15625 | .14063 | .17188 | .19531 | .24609 | .18359 |
| $R_1$ | .01134 | .01025 | .00948 | .00768 | .00986 | .01007 | .00928 | .01064 |
| $R_2$ | .01505 | .01425 | .01339 | .01150 | .01564 | .01634 | .01530 | .01512 |
| $r$ | .07422 | .08984 | .07813 | .06641 | .08984 | .13672 | .11328 | .07813 |

Table 4: Approximation error for 4 times compression of the function $f_{(4,3)}$.

In Fig. 7. the recovery of a "rough" source function $f_{(5,2)}$ is depicted after compression of different transform coding. It is difficult to judge visually for the quality of the different recoveries. The quantitative measures for the quality of the recoveries of the source function from Fig. 7. are given in Table 4. for 4 times compression, and in Table 5. for 16 times compression.

From Table 4 it is seen that for 4 times compression the smallest error for all distances is for the fractal transform coding $F(.50)$.

For 16 times compression (Table 4) the best method for $l_1$ and $l_2$ is the Haar one, for $l_\infty$ is $F(.25)$, for integral Hausdorff distances $R_1$ and $R_2$ is $F(-.75)$, and for the Hausdorff distance $r$ is $F(.25)$.

For the other "rough" source functions the best methods differ.

The dependence of the approximation error, with respect to different distances, from the fractalization parameter $\lambda$ for different compression factors is very irregular. One fractalization parameter for all levels of a function is not a natural way for approximation of "rough" functions.

| | H | EH | F(.25) | F(.50) | F(.75) | F(-.75) | F(-.50) | F(-.25) |
|---|---|---|---|---|---|---|---|---|
| $l_1$ | .06979 | .07523 | .08113 | .08612 | .10007 | .09631 | .08696 | .07538 |
| $l_2$ | .10364 | .10750 | .11042 | .11325 | .12654 | .12735 | .11327 | .10608 |
| $l_\infty$ | .46094 | .45313 | .35938 | .41016 | .41016 | .39063 | .40234 | .44531 |
| $R_1$ | .03168 | .02818 | .02493 | .02333 | .02666 | .02010 | .02644 | .02661 |
| $R_2$ | .04326 | .04088 | .03819 | .03465 | .04094 | .03152 | .03991 | .04040 |
| $r$ | .21875 | .19531 | .17188 | .21875 | .21875 | .20703 | .20703 | .21484 |

Table 5: Approximation error for 16 times compression of the function $f_{(4,3)}$.

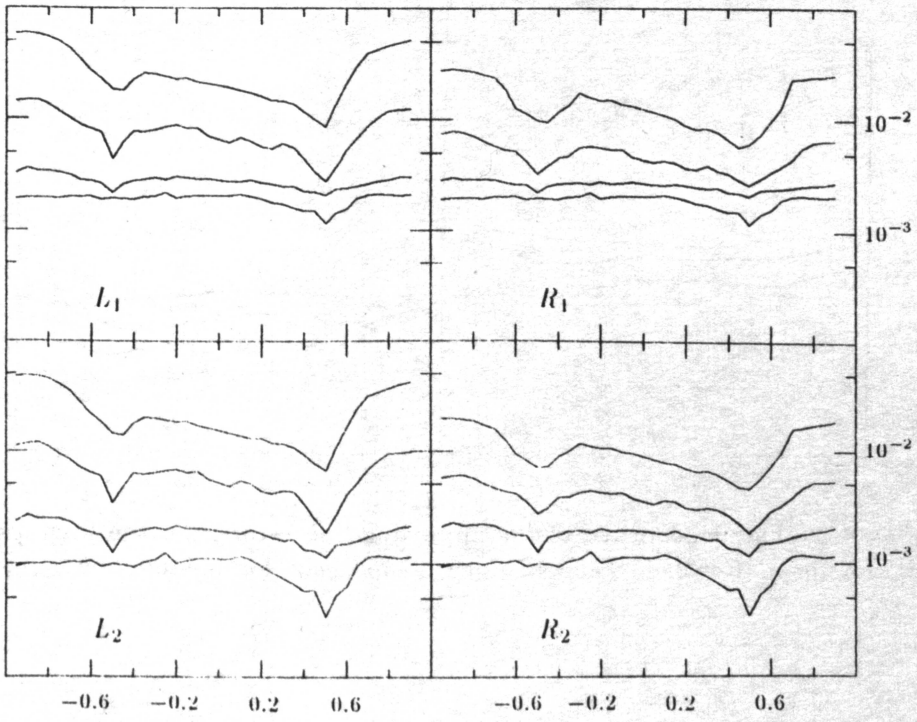


Figure 8: The dependence of the approximation error from the fractalization parameter $\lambda$ after 2, 4, 8 and 16 times compression for the function $f_{(1,2)}$.

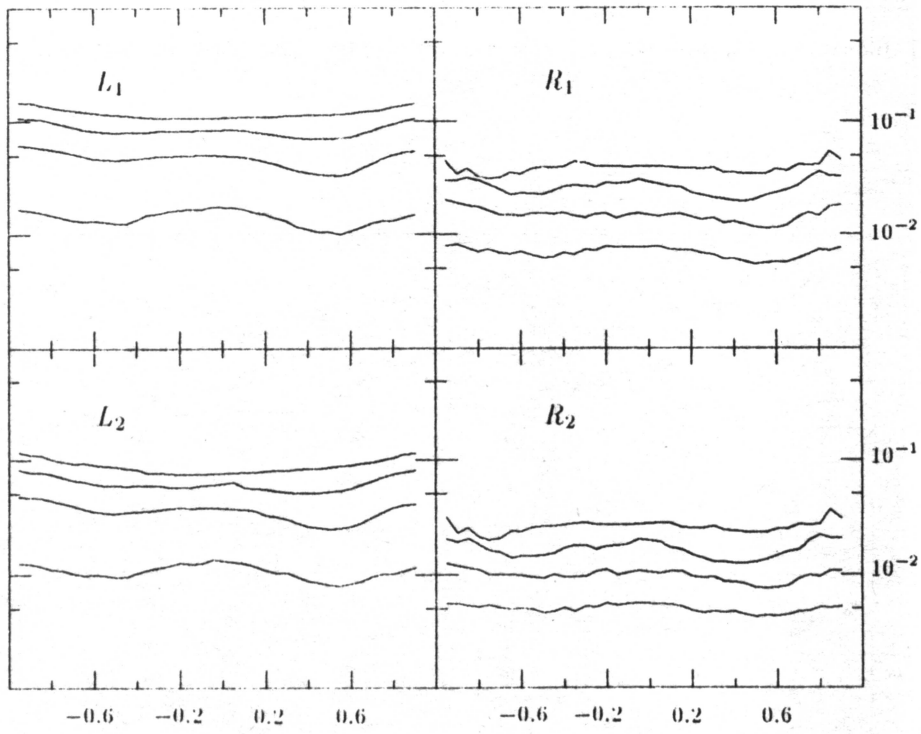


Figure 9: The dependence of the approximation error from the fractalization parameter $\lambda$ after 2, 4, 8 and 16 times compression for the function $f_{(4,3)}$.

In Fig. 8 four graphics of the error as a function of the fractalization factor are presented for 2, 4, 8, and 16 times compression of the smooth source function $f_{(1,2)}$. In all cases the smallest error is for $\lambda = 0.5$, but there are many local minima.

The same graphics are presented in Fig. 9 for the "rough" source function $f_{(4,3)}$. There are absolute minima for different values of the fractalization parameter and there are many local minima.

Remark 6.2. The same theory is valid for the $m$-dimensional unit cube. Computer experiments for approximation and compression of images ($m = 2$) will be considered in a forthcoming paper.

## References


[1] M. F. Barnsley. *Fractals Everywhere*, Boston, 1988.

[2] M. F. Barnsley, J. H. Elton and D. P. Hardin. Recurrent iterated function systems, *Constr. Approx.*, **5**, 1989, 3 - 31.

[3] M. F. Barnsley, J. H. Elton, D. Hardin and P. Massopust. Hiden variable fractal interpolation functions, *SIAM J. Math. Anal.*, **20**, 1989, 1218 - 1242.

[4] M. F. Barnsley and L. P. Hurd. *Fractal Image Compression*, AK Peters, Ltd. Wellesley, Massachusetts, 1993.

[5] T. Bedford. On Weierstrass-like functions and random recurrent sets, *Proc. Cambr. Phil. Soc.*, **106**, 1989, no. 2, 325 - 342.

[6] A. Deliu and B. Jawerth. Geometrical dimension versus smoothness, *Constr. Approx.*, **8**, 1992, 211 - 222.

[7] A. Deliu, J. S. Geronimo, R. Shonkwiler and D. Hardin. Dimensions associated with recurrent self-similar sets, *Math. Proc. Cambridge Philos. Soc.*, **110**, 1991, 327 - 336.

[8] K. J. Falconer, The Hausdorff dimension of self-affine fractals, *Math. Proc. Cambridge Philos. Soc.*, **103**, 1988, no. 2, 339 - 350.

[9] D. P. Hardin, B. Kessler, and P. R. Massopust. Multiresolution analysis based on fractal functions, *J. of Approximation Theory*, **71**, 1992, 104 - 120.

[10] G. H. Hardy. Weierstrass's nondifferentiable function, *Trans. Amer. Math. Soc.*, **17**, 1916, 322 - 323.

[11] M. Hata. On the structure of the self-similar sets, *Japan J. Appl. Math.*,**2**, 1985, 381 - 414.

[12] F. Hausdorff. *Mengenlehre*, W. Gruyter & Co., Berlin, 1927.

[13] Tian You Hu and Ka-Sing Lau. Fractals dimension and singularities of the waierstrass type functions, *Trans. Amer. Math. Soc.*, **335**, 1993, no. 2, 649 - 665.

[14] J. E. Hutchinson. Fractals and self similarity, *Indiana Univ. Math. J.*, **30**, 1981, 713 - 747.

[15] G. B. Lewellen. Self-similarity, *Rocky Mountain J. of Math.*, 3, **23**, 1992, 1023 - 1040.

[16] B. B. Mandelbrot. *The Fractal Geometry of Nature*, San Francisco, Freeman, 1982.

[17] P. Maragos and Fang-Kuo Sun. Measuring the fractal dimension of ssignals: Morphological covers and iterative optimization, *IEEE Trans. on Signal Processing*, **41**, 1993, 108 - 119.

[18] Bl. Sendov. Mathematical modeling of real-world images, *Constr. Approx.*, 1996.

[19] Bl. Sendov. *Hausdorff Approximations*, Kluwer Academic Publishers, Dordrecht / Boston / London, 1990.

[20] Bl. Sendov. Integral Hausdorff metric, *CR l'Acad. bulgare de Sci.*, **46**, 1993, no. 10, 21 - 24.

[21] Dao Shun Sun and Jia Rong Yu. Bouligand dimension of some fractals represented by lacunary or random lacunary trigonometric series, *Sci. China Ser. A*, **35**, 1992, 426 - 436.

[22] M. D. Takev. On the Hausdorff dimension of completed graphs, *CR l'Acad. bulgare de Sci.*, **45**, 1992, no. 7, 13 - 15.

*Central Laboratory for Parallel Processing*
*Bulgarian Academy of Sciences*
*"Acad. G. Bonchev" street, Block 25A,*
*1113 Sofia, BULGARIA*
*E-mail: sendov@amigo.acad.bg*

*Received 23.03.1996*